View metadata, citation and similar papers at core.ac.uk
brought to you by CORE

東北大学機関リポジトリ
TOUR
Tohoku University Repository

Large-rotation and low-voltage driving of micromirror realized by tense thin-film torsion bar

著者	羽根　一博
journal or publication title	IEEE photonics technology letters
volume	18
number	15
page range	1573-1575
year	2006
URL	http://hdl.handle.net/10097/35132

doi: 10.1109/LPT.2006.879587

Large-Rotation and Low-Voltage Driving of Micromirror Realized by Tense Thin-Film Torsion Bar

Minoru Sasaki, Shinya Yuki, and Kazuhiro Hane

***Abstract*—An electrostatically driven micromirror device using a thin-film torsion bar is proposed. The mirror rotation angle of 7.3° at 5 V is demonstrated at the nonresonant condition. A bulk Si micromirror is suspended by SiN thin-film torsion bars. Inside the torsion bar, the tension having the magnitude larger than that of the driving force is included. The torsion bar can have a compliance with the mirror rotation and the rigidity against the unwanted motions (e.g., vertical displacement or in-plane rotation).**

***Index Terms*—Electrostatic driving, low-voltage driving, micromirror, tension, thin-film torsion bar.**

I. Introduction

THE electrostatic driving is frequently used for micromirror devices, since it has the advantage of low power consumption. The heat generation and the resultant degradation of the device reliability can be prevented. The highly integrated mirror array prefers the electrostatic driving. The limitation of electrostatic driving is the difficulty for obtaining the large rotation angle with the low voltage driving.

Fundamentally, there are two methods for decreasing the driving voltage. One is increasing the driving force. Another is decreasing the spring constant. One micromirror is prepared by the surface micromachining adopting both methods [1]. In general, the torsion bar is frequently designed as the serpentine spring. The folded bar will be softer not only for rotation, but also for vertical and in-plain displacement and rotation. The resultant mirror motion depends on the balance of the spring constants for many modes of the mirror motion [2]. The spring constant for the mirror rotation should be minimized while maintaining the rigidity in other motions. The serpentine spring helps the design, but often does not completely solve the problem [3]. A group of Lucent Technologies reports a design with the so-called bearings for supporting the torsion bar against the vertical displacement [4]. As a new bearing material, a double wall carbon nano-tube is tested [5]. A group of Fujitsu adopted the V-shape torsion bar, which is robust against the in-plane rotation [6]. Taking advantage of this, the thick vertical combs can generate a larger driving force.

In this study, the thin-film torsion bar is proposed for decreasing the rotational spring constant and the driving voltage [7], [8]. The tension is included inside the torsion bar for increasing the rigidity against the unwanted mirror motion.

Manuscript received March 6, 2006; revised May 8, 2006. The facilities used for this research include the Venture Business Laboratory at Tohoku University.

The authors are with the Department of Nanomechanics, Tohoku University, Sendai, 980-8579, Japan (e-mail: sasaki@hane.mech.tohoku.ac.jp).

Digital Object Identifier 10.1109/LPT.2006.879587

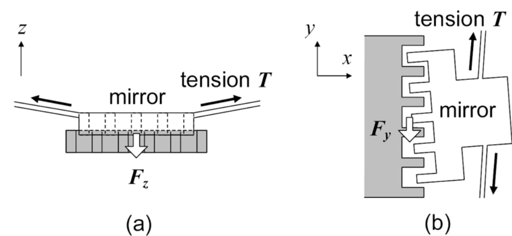

Fig. 1. Effects of tension inside the torsion bar for suppressing unwanted mirror motions.

II. Principle

Supposing the rectangular cross section of the torsion bar, the torsional spring constant k_θ is expressed as follows:

$$k_\theta \approx \frac{Gwt^3}{3l}\left(1 - \frac{192}{\pi}\frac{t}{w}\tanh\frac{\pi w}{2t}\right) \quad (1)$$

where G is the shear modulus, l is the length of torsion bar, and w and t are width or thickness, supposing the relation of $w > t$. When thin films are considered, t is the thickness. The factor t^3 shows that decreasing the value t is effective for decreasing k_θ. When the proximity patterning is considered, the minimum pattern size is a few micrometers. Considering the deposited thin film, the thickness of a few 100 nm can be obtained. The estimated spring constant from (1) is 1.4×10^{-11} Nm/rad by setting values of G, l, w, and t as 80 GPa, 200, 4, and 0.3 μm, respectively.

The torsion bar needs a low spring constant for twisting motion while needing high spring constants for other modes. To achieve this, tension is applied to the torsion bar. As can be seen from Fig. 1(a), the tension works against the vertical displacement of the mirror. The tensile stress σ_0 inside SiN film can be 760 MPa [9], the tension $T = \sigma_0 wt$ is 910 μN for $4 \times 0.3\ \mu\text{m}^2$ cross section. This value is large compared to the driving force of about 7 nN in our actuator design. Since the thin-film torsion bar is softest in the vertical direction, the vertical spring constant k_z is most important. k_z is expressed as follows [10]:

$$k_z \approx \frac{1}{\sum_{n=1,\text{odd}}^{\infty} \frac{1}{l}\frac{2}{\frac{Ewt^3}{12}k_n^4 + \sigma_0 wt k_n^2}}$$
$$k_n = \frac{n\pi}{l} \quad (n = 1, 3, 5, \ldots). \quad (2)$$

There are terms correspond to the factors due to the elasticity E (290 GPa) and the stress σ_0. Considering the term corre-

1041-1135/$20.00 © 2006 IEEE

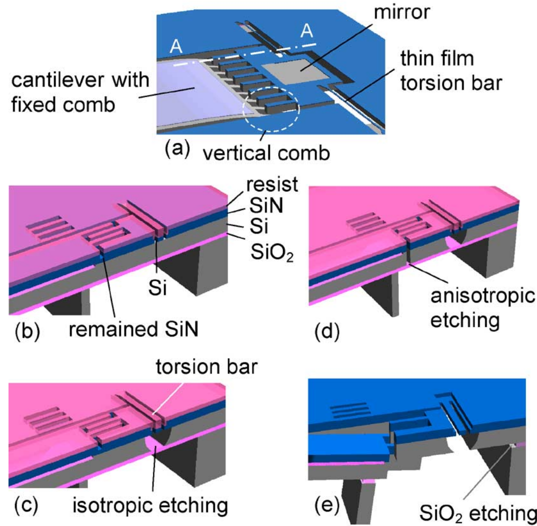

Fig. 2. (a) Schematic of the mirror device. (b)–(e) Fabrication sequence for preparing the thin-film torsion bar showing A-A cross section. (Color version available online at http://ieeexplore.ieee.org.)

sponding to $n = 1$, k_z are 0.016 and 23 N/m when σ_0 is 0 and 760 MPa, respectively. The large spring constant suppresses the vertical displacement of the mirror. The increase of the torsional spring constant $\Delta k_{\theta\text{stretch}}$ generated by the beam stretching can be estimated as follows:

$$\Delta k_{\theta\ \text{stretch}} \approx \frac{1}{8l}\left\{\frac{\sigma_0(w^3t + wt^3)}{3} + \frac{E}{2l^2}\left(\frac{w^5t}{10} + \frac{w^3t^3}{9} + \frac{wt^5}{10}\right)\theta^2\right\}. \quad (3)$$

The first term corresponds to stretching against the stress σ_0. The second nonlinear part corresponds to the elastic stretching. The dominant part is the first term having the value of 3.1×10^{-12} Nm/rad when the mirror rotation is small (<6.6 rad). This is 22% of the spring constant estimated from (1). The tension is fundamentally perpendicular to the rotational displacement of the material inside the torsion bar. The increase of the spring constant is minimized. Fig. 1(b) shows the case when the comb drive actuator generates the unbalanced force and the torque inducing the in-plane rotation of the mirror. Again the tension works against this mirror motion.

III. Preparation of Thin-Film Torsion Bar

Fig. 2(a) shows a schematic of the micromirror. The moving comb is attached to the mirror. The fixed comb is at the end of the cantilever. Fig. 2(b)–(e) illustrates the fabrication sequence for the torsion bar showing A-A cross section in Fig. 2(a). A silicon-on-insulator wafer is used. The thicknesses of device Si, buried oxide, and handling Si are 10, 2, and 200 μm, respectively. The structures of the thin-film torsion bar and the vertical comb drive actuator are realized by combining the isotropic and the anisotropic Si plasma etching. SiN film is patterned by the resist masks, as shown in Fig. 2(b). There is no SiN film in the region around the torsion bar, whereas the other region has the SiN film. The Si layer around the torsion bar is underetched and the thin-film torsion bar is released from the substrate using the photoresist and the SiN film masks [Fig. 2(c)]. After SiN masking

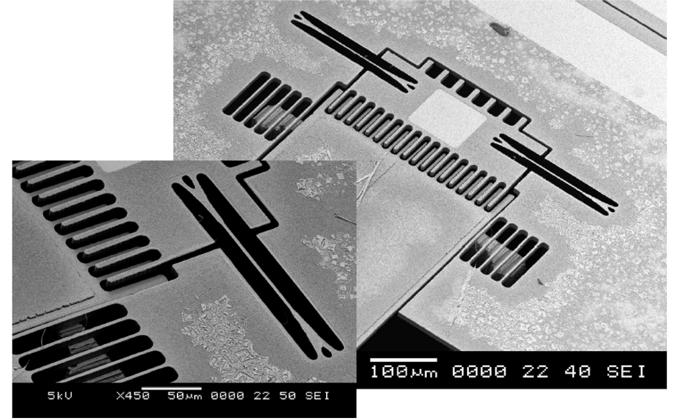

Fig. 3. Fabricated micromirror and the magnified image of the torsion bar and the vertical comb.

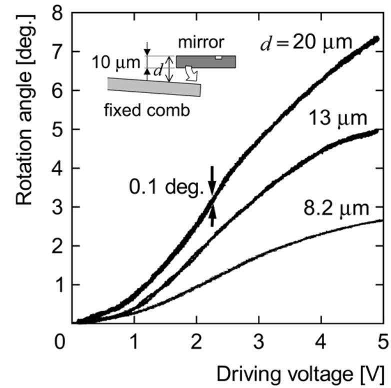

Fig. 4. Mirror rotation as a function of the driving voltage. Rotation angle is measured using the optical lever method. Parameter d is the comb-to-comb vertical distance at the initial state. The schematic shows the side view of the vertical combs.

layer is removed, the anisotropic Si etching is carried out. The comb and the mirror structures with the vertical sidewall are fabricated [Fig. 2(d)]. The sacrificial SiO_2 layer is etched and the mirror is released. The photoresist mask remains through the process. The fixed comb is at the end of the cantilever with SiO_2 film as shown in Fig. 2(a). The cantilever deflects downward due to the compress stress in SiO_2 film [Fig. 2(e)] [11]. SiO_2 film is thermally grown at the beginning of the process and covered by the thin SiN film. After removing the photoresist, Au–Cr is deposited over the wafer for the electrical connection across insulating torsion bar. Fig. 3 shows a fabricated micromirror. The square mirror size is $100 \times 100\ \mu\text{m}^2$. This area is free from SiN insulation layer and the electrical connection to the bulk mirror is obtained. The magnified image shows the torsion bar and the vertical comb. The dimensions of the torsion bar are $200 \times 4 \times 0.3\ \mu\text{m}^3$.

IV. Results

Fig. 4 shows the mirror rotation angle as a function of the driving voltage. The mirror is grounded and the fixed comb is biased. The comb-to-comb height difference d at the initial state is the parameter. Three different devices are measured. With the increase of d from 8.2 to 20 μm, the mirror rotation angle increases. The curves change from the concave up to down with increasing driving voltage. The thickness of the comb finger is

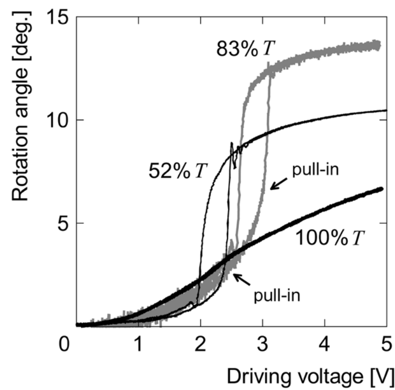

Fig. 5. Mirror rotation as a function of the driving voltage. d is 20 μm. Thick black, thick gray, and thin black curves correspond to 100%, 83%, and 52% of the original tension T in the bar, respectively.

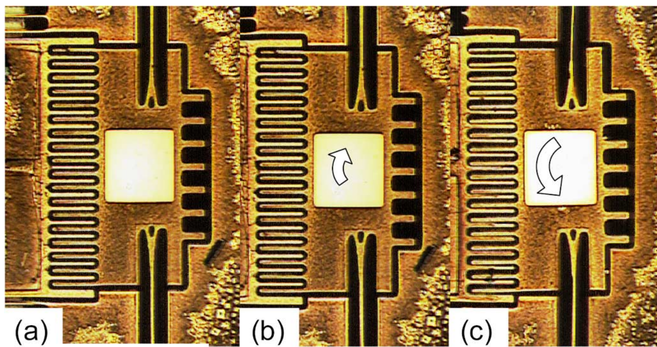

Fig. 6. Micromirror suspended by the torsion bars with 100% tension at the driving voltage of (a) 50 and (b) 80 V. (c) Torsion bars with 52% tension at the driving voltage of 35 V. (Color version available online at http://ieeexplore.ieee.org.)

10 μm. The mirror with d of 8.2 μm has the overlap of 1.8 μm between combs at the initial state. The mirrors with d of 13 and 20 μm have initial gaps. When d is 20 μm, the rotation angle reaches 7.3° at 5 V. The comb gap is 4 μm in the lateral direction. The curve is smooth showing a nearly linear relation compared with that obtained from the device with 0.5-μm gap in [1]. Fig. 4 shows a round-trip data. The hysteresis (defined by the maximum difference of the rotation angle at the same driving voltage in the round trip motion) is 0.1°. The resonance frequency of the mirror is about 670 Hz.

The relation between the performance of the mirror device and the tension inside the torsion bar is investigated. The tension is decreased by the compress stress added by the implantation of boron ion in the film. The stress values are monitored using a strain gauge [12]. Supposing the Young's modulus E of SiN film to be 290 GPa [13], the estimated original stress is 780 MPa. When the dose is 3.2×10^{14} atoms/cm^2 at the acceleration of 70 keV, the tensile stress decreases to 83% of the origial value. With the additional dose of 1.0×10^{15} atoms/cm^2 at 130 keV to the same wafer, the stress decreases to 52% of the origial value.

Fig. 5 shows the mirror rotation angle as a function of the driving voltage. The distance d is 20 μm. With the decrease of the tension, S-shape of the curve, and the pull-in phenomenon becomes more pronounced and the hysteresis in the round-trip motion becomes larger. The pull-in voltages are 3.0 and 2.4 V for 83% and 52% tension T, respectively. The stably obtainable rotaion angle before the pull-in is limitted to 7° and 4° for 83% and 52% tension, respectively. At the relatively small driving voltage around 2 V, the torsion bar with the original 100% tension shows the largest rotation angle. With the decrease of the tension, the larger vertical displacement of the mirror is considered to be generated decreasing the mirror rotation.

The side snap over (unstable in-plane rotation) is measured. Fig. 6(a) and (b) shows images when the driving voltages are 50 and 80 V, respectively. The tension is originally 100%. The mirror is stable at 50 V, and the in-plane rotation is slightly observed at 80 V. Fig. 5(c) shows the case when the side snap over occurs at 35 V with 52% tension in the torsion bar.

REFERENCES

[1] D. Hah, S. T. Huang, J. Tsai, H. Toshiyoshi, and M. C. Wu, "Low-voltage, large-scan angle MEMS analog micromirror arrays with hidden vertical comb-drive actuators," *J. Microelectromech. Syst.*, vol. 13, pp. 279–289, Apr. 2004.

[2] T. D. Kudrle, C. C. Wang, M. G. Bancu, J. C. Hsiao, A. Pareek, M. Waelti, G. A. Kirkos, T. Shone, C. D. Fung, and C. H. Mastrangelo, "Single-crystal silicon micromirror array with polysilicon flexures," *Sens. Actuators*, vol. A119, pp. 559–566, Apr. 2005.

[3] G. Barillaro, A. Molfese, A. Nannini, and F. Pieri, "Analysis, simulation and relative performance of two kinds of serpentine springs," *J. Micromech. Microeng.*, vol. 15, pp. 736–746, Feb. 2005.

[4] V. A. Aksyuk, F. Pardo, D. Carr, D. Greywall, H. B. Chan, M. E. Simon, A. Gasparyan, H. Shea, V. Lifton, C. Bolle, S. Arney, R. Frahm, M. Paczkowski, M. Haueis, R. Ryf, D. T. Neilson, J. Kim, C. R. Giles, and D. Bishop, "Beam-steering micromirrors for large optical crossconnects," *J. Lightw. Technol.*, vol. 21, no. 3, pp. 634–642, Mar. 2003.

[5] A. M. Fennimore, T. D. Yuzvinsky, W.-Q. Han, M. S. Fuhrer, J. Cuming, and A. Zettl, "Rotational actuators based on carbon nanotubes," *Nature*, vol. 424, pp. 408–410, Jul. 2003.

[6] M. Yano, F. Yamagishi, and T. Tsuda, "Optical MEMS for photonic switching-compact and stable optical crossconnect switches for simple, fast, and flexible wavelength applications in recent photonic networks," *IEEE J. Sel. Topics Quantum Electron.*, vol. 11, no. 2, pp. 383–394, Mar./Apr. 2005.

[7] S. Yuuki, M. Sasaki, and K. Hane, "Large-rotation and low-voltage driving realized by micromirror with vertical comb and tense thin film torsion bar," in *Proc. 13th Int. Conf. Solid-State Sensors, Actuators and Microsystems*, 2005, vol. 3A2.1, pp. 1163–1166.

[8] M. Sasaki, S. Yuuki, and K. Hane, "Performance of tense thin film torsion bar for large-rotation and low-voltage driving of micromirror," in *Proc. Int. Conf. Optical MEMS and Their Applications 2005*, 2005, vol. H5, pp. 129–130.

[9] M. Sekimoto, H. Yoshihara, T. Ohkubo, and Y. Saitoh, "Silicon nitride single-layer X-ray mask," *Jpn. J. Appl. Phys.*, vol. 20, pp. L669–L672, Sep. 1981.

[10] S. D. Senturia, *Microsystem Design*. New York: Springer, ch. 9.

[11] M. Sasaki, D. Briand, W. Noell, N. de Rooij, and K. Hane, "Three-dimensional SOI-MEMS constructed by buckled bridges and vertical comb drive actuator," *IEEE J. Sel. Topics Quantum Electron.*, vol. 10, no. 3, pp. 455–461, May/Jun. 2004.

[12] L. Lin, A. P. Pisano, and R. T. Howe, "A micro strain gauge with mechanical amplifier," *J. Microelectromech. Syst.*, vol. 6, pp. 313–321, Dec. 1997.

[13] O. Tabata, K. Kawahata, S. Sugiyama, and I. Igarashi, "Mechanical property measurements of thin films using load-deflection of composite rectangular membranes," *Sens. Actuators*, vol. 20, pp. 135–141, Nov. 1989.